AIAA JOURNAL
Vol. 46, No. 6, June 2008

Sensitivity Analysis Method for Membrane Wrinkling Based on the Tension-Field Theory

Takeshi Akita*
Osaka Prefecture University, Osaka 599-8531, Japan
and
M. C. Natori†
Japan Aerospace Exploration Agency, Kanagawa 229-8510, Japan.

DOI: 10.2514/1.33187

This paper presents a new method for the sensitivity analysis of membrane wrinkling based on the tension-field theory. This method can be applied to design membrane structures to reduce the occurrence of wrinkles. In this method, the wrinkle intensity in a partly wrinkled membrane is evaluated from an apparent strain energy resulting from the deformation through wrinkling. This wrinkle intensity is used as an objective function for wrinkle-reduction membrane design. Further, the sensitivity of the wrinkle intensity with respect to an arbitrary design parameter is derived by employing a semi-analytical differentiation technique and is used to resolve the minimization problem of the objective function. Some design examples show that this minimization problem can be effectively resolved by the proposed sensitivity analysis method and the occurrence of membrane wrinkles can be considerably reduced by minimizing the wrinkle intensity.

Nomenclature

a_c	=	small constant value for the incremental line search
$\mathbf{B}_L^k$	=	strain-displacement relation matrix of the kth element
$\mathbf{b}$	=	design parameter vector
b_j	=	jth design parameter
$\mathbf{C}$	=	elasticity matrix for the membrane
$\mathbf{C}_m$	=	modified elasticity matrix for the wrinkled membrane
E	=	Young's modulus
$\mathbf{K}$	=	tangent stiffness matrix in the equilibrium state
$\mathbf{n}_1, \mathbf{n}_2$	=	vectors for coordinate transformation of stress
$\mathbf{P}, \mathbf{Q}$	=	projection matrices
$\mathbf{q}$	=	internal force vector in the equilibrium state
r	=	penalty coefficient for the area constraint
S	=	membrane area
S_0	=	initial membrane area
s	=	step variable for the incremental line search
$\mathbf{s}_1, \mathbf{s}_2$	=	vectors for coordinate transformation of the strain
U_s	=	penalty function for the area constraint
U_w	=	total wrinkle intensity over the entire membrane
U_w^k	=	wrinkle intensity over the kth membrane element
w^k	=	weight coefficient for U_w^k
β	=	minute perturbation for numerical differentiation
γ	=	minimum value of the ratio of the required membrane area to S_0
Δb_j	=	numerical perturbation of b_j
ΔU_w	=	numerical perturbation of U_w
$\boldsymbol{\varepsilon}$	=	strain vector in the plane stress state
$\boldsymbol{\varepsilon}_e$	=	elastic strain vector
$\boldsymbol{\varepsilon}_w$	=	wrinkle-mode deformation vector
$\varepsilon_x, \varepsilon_y, \gamma_{xy}$	=	strain components in the x–y coordinate system
$\varepsilon_1, \varepsilon_2$	=	major and minor principal strains, respectively
ε_{2w}	=	nonzero scalar value contained in $\boldsymbol{\varepsilon}_w$
θ	=	rotation angle of principal axes of stress and strain tensors to the x–y axes
ν	=	Poisson's ratio
$\boldsymbol{\sigma}$	=	stress vector in the plane stress state
$\boldsymbol{\sigma}_t$	=	uniaxial tensile stress vector in the wrinkled membrane
$\sigma_x, \sigma_y, \tau_{xy}$	=	stress components in the x–y coordinate system
σ_1, σ_2	=	major and minor principal stresses, respectively
ϕ_e	=	strain energy density in a wrinkled membrane
ϕ_p	=	strain energy density in a taut membrane
ϕ_w	=	wrinkle intensity at a material point
φ	=	augmented objective function for shape optimization

Introduction

IN RECENT times, membranes have attracted considerable interest in the field of space structure engineering due to their high packaging efficiency and low weight. Because membranes have little resistance to compressive stresses, wrinkles may appear over partial or entire regions. Such wrinkles could cause significant deterioration in the performance of membrane structures. For example, the occurrence of wrinkles could reduce surface accuracy in membrane reflectors [1] or cause nonuniform surface heating in solar sails [2]. Therefore, the design of efficient membrane structures that would minimize wrinkle occurrence is of tremendous importance.

In the design of membrane structures on the ground, wrinkling is usually avoided by designing membrane surfaces as minimal surfaces on which equal tension fields are developed within given boundaries [3,4]. For space membrane structures such as solar sails, catenary system designs (in which catenary cables are installed along the membrane boundaries to provide uniform tension) are often used [5–7]. Theoretically, these surface or boundary designs can realize wrinkle-free taut conditions over entire membrane surfaces; however, the shapes of membrane surfaces obtained are considerably restricted. Such shape restrictions could be undesirable in some cases, for example, to achieve various mission objectives of space

Presented as Paper 1800 at the 47th AIAA/ASME/ASCE/AHS/ASC Structures, Structural Dynamics, and Materials Conference, Newport, RI, 1–4 May 2006; received 2 July 2007; revision received 18 December 2007; accepted for publication 18 December 2007.

*Assistant Professor, Department of Aerospace Engineering, 1-1 Gakuencho, Sakai; akita@aero.osakafu-u.ac.jp. Member AIAA.

†Professor Emeritus, Institute of Space and Astronautical Science; currently Visiting Professor, Advanced Research Institute for Science and Engineering, Waseda University, 3-4-1 Okubo, Room 55S-06-08A, Shinjyuku-ku, Tokyo 169-8555. Associate Fellow AIAA.

structures. In addition, it is often sufficient to eliminate only those wrinkles that exist near a critical area of mission performance. Recently, some researchers have studied another boundary design for wrinkle reduction in which shear compliant borders are integrated along the edges of flat membranes of solar sails [2,8]. To produce feasible designs for various types of space membrane structures, another design approach that tolerates some insignificant wrinkles on the membranes is widely used [9,10]. In this approach, a feasible wrinkle-tolerant membrane design is obtained by numerical analysis based on the tension-field (TF) theory, which can predict the locations of wrinkled regions in partly wrinkled membranes. If wrinkled regions exist near critical areas of mission performance, they can be separated from those areas by tuning some design parameters. Generally, large computational costs are incurred when obtaining optimum parameters because they are usually found by trial-and-error methods. To apply a usual optimization scheme for an efficient parameter search, evaluations of wrinkle intensity and its sensitivity are essentially required; however, for the existing techniques based on TF theory, such evaluations are difficult.

The aim of this paper is to offer a new sensitivity analysis method for membrane wrinkling; this method evaluates both wrinkle intensity and its sensitivity based on the TF theory. In the proposed method, a wrinkled membrane is modeled via a projection technique [11,12] that provides a simple treatment of wrinkle phenomenon. Subsequently, we introduce a quantifier that represents the intensity of membrane wrinkling at a material point from the viewpoint of strain energy density. This quantifier depends on only the deformation caused by wrinkling and can be systematically defined by using the projection technique. The total intensity of membrane wrinkling over the entire membrane is defined by the numerical integrals of the quantifier on the discretized membrane surface; further, its sensitivity with respect to an arbitrary design parameter is efficiently obtained by the semi-analytical differentiation method (SDM) [13,14]. These quantities can be easily evaluated in conjunction with a nonlinear finite element method. To obtain a wrinkle-reduction membrane design, we consider the minimization problem of the total intensity of membrane wrinkling with respect to arbitrary design parameters. Such minimization problems can be resolved by general optimization schemes with the sensitivity analysis method presented in this paper. Some numerical examples are shown to demonstrate the accuracy and effectiveness of the proposed method.

Modeling of Wrinkled Membranes Based on the TF Theory

The pioneering work on the TF theory was performed by Wagner [15], and since then there have been numerous studies concerning wrinkling analysis based on the TF theory (see [16] and the references therein). Since the early 1970s, a considerable amount of research has been conducted on the numerical analysis of wrinkled membranes. In most of these studies, the wrinkling phenomenon is modeled by modifying the stress–strain relations of wrinkled membranes. Miller et al. [17] proposed a modified elasticity matrix that represents the stress–strain relations in wrinkled membranes. The modified matrix was incorporated into a few commercial finite element method codes [18] and has been used for the design of space membrane structures [9,10]. Some approaches similar to that of Miller are presented in [19–22]. Ding et al. [23,24] developed a numerical analysis method that copes with a variable Poisson's ratio [25,26] by using an optimization technique. Contri and Schrefler [27] proposed a simple procedure in which the residual forces are modified to model no-compression material properties of wrinkled membranes in geometrically nonlinear problems. Pipkin [28] and Steigmann and Pipkin [29] generalized the TF theory by deriving a relaxed energy density for membrane deformations. Some researchers have conducted numerical analysis of wrinkled membranes based on the relaxed energy densities [30–33]. Wu and Canfield [34] proposed another model for wrinkled membranes in which deformation gradient tensors are modified to represent the TF responses of wrinkled membranes. Roddeman et al. [35,36] extended the model to anisotropic membranes and large deformation problems. Since then, several researchers have applied the Roddeman model to the finite element analysis of wrinkled membranes [37–42]. Recently, Nakashino and Natori [43,44] presented a simple calculation scheme for the Roddeman model by deriving the modified elasticity tensor that is consistent with the modified deformation tensor. Further, the authors have investigated the modified elasticity tensor from the viewpoint of linear algebra and have presented an efficient modeling technique for wrinkle behavior via a projection technique [11,12]. Miyazaki [45] reviewed the various wrinkle models proposed in the literature and proposed a new scheme for the nonlinear dynamic analysis of wrinkled/slackened membranes.

In this paper, a wrinkled membrane is modeled via a projection technique [11,12] that provides a simple treatment for wrinkle phenomenon. In this wrinkle model, a sequence of two deformation processes for total deformation in a wrinkled membrane is considered: an elastic deformation followed by zero-strain energy deformation due to wrinkling. Through this sequence, the total strain in the wrinkled membrane is decomposed into two parts: a pure elastic strain part and a zero-strain energy part resulting from deformation through wrinkling. Then projection matrices that decompose the total strain into the elastic part and zero-strain energy part are derived. A review and some remarks on the wrinkle model based on the projection technique are provided in this section.

Basic Assumptions of the TF Theory

We start from a review of the basic assumptions of the TF theory. In the TF theory, a structure idealized as a membrane is with zero flexural stiffness, and it cannot sustain any compressive stresses. When compressive stresses are about to appear in the membrane, they are immediately released by out-of-plane deformations (that is, the membrane wrinkles), as shown in Fig. 1a. The stress field after wrinkling is modeled as a uniaxial tension field, in which one principal stress is tensile and the other is zero, and the direction of wrinkle is assumed to be identical to that of the tension lines. In addition, the out-of-plane deformation caused by wrinkling is replaced by the in-plane contraction, the direction of which is perpendicular to that of wrinkles, as shown in Fig. 1b. In isotropic membranes, such in-plane contraction is the zero-energy deformation because its direction coincides with the principal axis corresponding to zero stress. In the TF theory, the wrinkled membrane can be treated as a planar problem, in that local buckling caused by wrinkling is simplified to the in-plane contraction.

Basic Equations of Isotropic Membrane

Here, we briefly describe the basic equations of membranes in a state of plane stress. In this paper, we assume that membranes are

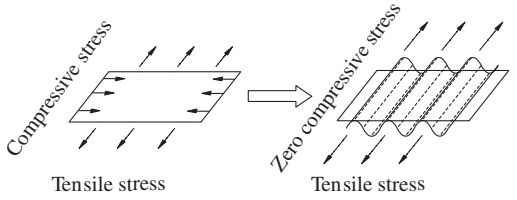

a) Uniaxial tension state

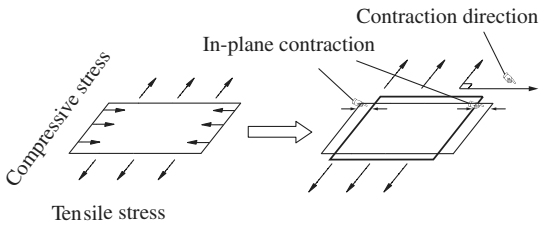

b) In-plane contraction

Fig. 1 Basic assumptions of the wrinkling model.

composed of isotropic elastic materials. Stress and strain components in an x–y coordinate system are represented as three-component column vectors:

$$\boldsymbol{\sigma} = [\sigma_x \quad \sigma_y \quad \tau_{xy}]^T, \qquad \boldsymbol{\varepsilon} = [\varepsilon_x \quad \varepsilon_y \quad \gamma_{xy}]^T \tag{1}$$

and the usual stress–strain relations are described via the elasticity matrix $\mathbf{C}$ as

$$\boldsymbol{\sigma} = \begin{bmatrix} \sigma_x \\ \sigma_y \\ \tau_{xy} \end{bmatrix} = \frac{E}{1-\nu^2} \begin{bmatrix} 1 & \nu & 0 \\ \nu & 1 & 0 \\ 0 & 0 & \frac{1-\nu}{2} \end{bmatrix} \begin{bmatrix} \varepsilon_x \\ \varepsilon_y \\ \gamma_{xy} \end{bmatrix} = \mathbf{C}\boldsymbol{\varepsilon} \tag{2}$$

where E is Young's modulus and ν is Poisson's ratio. Next, we consider a principal coordinate system rotated through an angle θ to the x–y axes. Then the usual coordinate transformation equations of stress and strain components are expressed in vector form, respectively, as follows:

$$\boldsymbol{\sigma} = \sigma_1 \mathbf{n}_1 + \sigma_2 \mathbf{n}_2 \tag{3}$$

$$\mathbf{n}_1 = [\cos^2\theta \quad \sin^2\theta \quad \sin\theta\cos\theta]^T \tag{4}$$

$$\mathbf{n}_2 = [\sin^2\theta \quad \cos^2\theta \quad -\sin\theta\cos\theta]^T \tag{5}$$

$$\boldsymbol{\varepsilon} = \varepsilon_1 \mathbf{s}_1 + \varepsilon_2 \mathbf{s}_2 \tag{6}$$

$$\mathbf{s}_1 = [\cos^2\theta \quad \sin^2\theta \quad 2\sin\theta\cos\theta]^T \tag{7}$$

$$\mathbf{s}_2 = [\sin^2\theta \quad \cos^2\theta \quad -2\sin\theta\cos\theta]^T \tag{8}$$

where σ_i and $\varepsilon_i (i = 1, 2)$ represent the principal stress and strain, respectively. In this paper, we assume $\sigma_1 > \sigma_2$ and $\varepsilon_1 > \varepsilon_2$. Finally, we introduce the vector $\mathbf{n}_3$ defined by

$$\mathbf{n}_3 \equiv \mathbf{n}_1 \times \mathbf{n}_2 \tag{9}$$

The inner product of Eqs. (3) and (9) leads to a relation between θ and $\boldsymbol{\varepsilon}$ as

$$f(\theta) = \mathbf{n}_3^T \boldsymbol{\sigma} = \mathbf{n}_3^T \mathbf{C}\boldsymbol{\varepsilon} = 0 \tag{10}$$

Wrinkle Model Based on a Projection Technique

In this subsection, we review the wrinkle model based on a projection technique [11,12] and make some remarks on the model. As mentioned before, in the TF theory, the out-of-plane deformation caused by wrinkling is replaced by the in-plane contraction that cannot be accounted for by the usual membrane theory. To account for the in-plane contraction, the deformed state of the wrinkled membrane is considered as a result of the sequence of two deformation processes [41], as shown in Fig. 2. Through this sequence, the total strain in the wrinkled membrane is decomposed into two parts: namely, a pure elastic strain part and a zero-strain energy part resulting from contraction of wrinkling. Now let σ_1 be the major principal value of the uniaxial tensile stress in the wrinkled membrane. In the first process, the membrane undergoes pure elastic deformation with the uniaxial tensile stress σ_1. By this deformation, the membrane is extended in the direction of the tensile stress and, at the same time, contracts in the perpendicular direction by Poisson's effect, as shown in Fig. 2a. We shall call the strain resulting from this deformation the elastic strain. In the second process, wrinkling brings about in-plane contraction, as shown in Fig. 2b, under the corresponding no-strain energy modes, as in the case of the TF theory. We call it a wrinkle-mode deformation. Through the sequence of these two processes, the total strain in the wrinkled membrane can be represented by the superimposition of the elastic strain and the wrinkle-mode deformation.

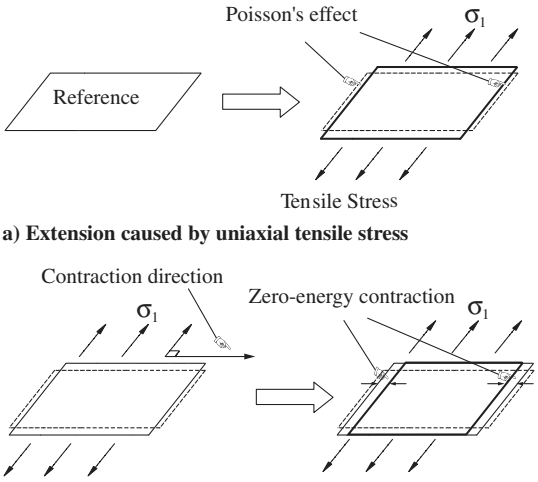

a) Extension caused by uniaxial tensile stress

b) Contraction caused by wrinkling

Fig. 2 Deformation process of wrinkling.

Next, we derive the elastic strain and the wrinkle-mode deformation in vectorial form. Using Eq. (3), the uniaxial stress vector $\boldsymbol{\sigma}_t$ in the wrinkled membrane can be expressed as

$$\boldsymbol{\sigma}_t = \sigma_1 \mathbf{n}_1 + 0\mathbf{n}_2 = \sigma_1 \mathbf{n}_1 \tag{11}$$

The assumption that the wrinkle-mode deformation produces no energy is represented by

$$\boldsymbol{\varepsilon}_w^T \boldsymbol{\sigma}_t = 0 \tag{12}$$

where $\boldsymbol{\varepsilon}_w$ is the wrinkle-mode deformation vector. Noting that the relation $\mathbf{s}_2^T \mathbf{n}_1 = 0$ holds, the wrinkle-mode deformation vector can be written with a nonzero scalar value ε_{2w} as

$$\boldsymbol{\varepsilon}_w = \varepsilon_{2w} \mathbf{s}_2 \tag{13}$$

Substituting Eqs. (11) and (13) into Eq. (12), we obtain

$$\boldsymbol{\varepsilon}_w^T \boldsymbol{\sigma}_t = (\varepsilon_{2w}\sigma_1)\mathbf{s}_2^T \mathbf{n}_1 = 0 \tag{14}$$

Now let $\boldsymbol{\varepsilon}$ be the total strain vector in the wrinkled membrane. Then the elastic strain vector $\boldsymbol{\varepsilon}_e$ is given by subtraction of $\boldsymbol{\varepsilon}_w$ from $\boldsymbol{\varepsilon}$ as

$$\boldsymbol{\varepsilon}_e = \boldsymbol{\varepsilon} - \boldsymbol{\varepsilon}_w = \boldsymbol{\varepsilon} - \varepsilon_{2w} \mathbf{s}_2 \tag{15}$$

Because $\boldsymbol{\varepsilon}_e$ consists of the pure elastic deformation, it is related to the uniaxial tensile stress vector $\boldsymbol{\sigma}_t$ by the usual elasticity matrix $\mathbf{C}$ as

$$\boldsymbol{\sigma}_t = \mathbf{C}\boldsymbol{\varepsilon}_e = \mathbf{C}(\boldsymbol{\varepsilon} - \varepsilon_{2w}\mathbf{s}_2) \tag{16}$$

Substituting Eqs. (13) and (16) into Eq. (12), we have

$$\varepsilon_{2w} \mathbf{s}_2^T \mathbf{C}(\boldsymbol{\varepsilon} - \varepsilon_{2w}\mathbf{s}_2) = 0 \tag{17}$$

The preceding equation is easily solved for ε_{2w} to yield

$$\varepsilon_{2w} = \frac{\mathbf{s}_2^T \mathbf{C}\boldsymbol{\varepsilon}}{\mathbf{s}_2^T \mathbf{C}\mathbf{s}_2} \tag{18}$$

Finally, substituting Eq. (18) into Eqs. (13) and (15) yields the vector expressions of $\boldsymbol{\varepsilon}_w$ and $\boldsymbol{\varepsilon}_e$, respectively, as follows:

$$\boldsymbol{\varepsilon}_w = \frac{\mathbf{s}_2^T \mathbf{C}\boldsymbol{\varepsilon}}{\mathbf{s}_2^T \mathbf{C}\mathbf{s}_2} \mathbf{s}_2 \tag{19}$$

$$\boldsymbol{\varepsilon}_e = \boldsymbol{\varepsilon} - \frac{\mathbf{s}_2^T \mathbf{C}\boldsymbol{\varepsilon}}{\mathbf{s}_2^T \mathbf{C}\mathbf{s}_2} \mathbf{s}_2 \tag{20}$$

The preceding vectors can also be presented in the matrix-vector form. It is easily proven that Eq. (19) can be rewritten in the matrix-vector form as

$$\boldsymbol{\varepsilon}_w = \frac{\mathbf{s}_2^T \mathbf{C} \boldsymbol{\varepsilon}}{\mathbf{s}_2^T \mathbf{C} \mathbf{s}_2} \mathbf{s}_2 = \mathbf{Q} \boldsymbol{\varepsilon} \tag{21}$$

where

$$\mathbf{Q} = \frac{\mathbf{s}_2 \mathbf{s}_2^T \mathbf{C}}{\mathbf{s}_2^T \mathbf{C} \mathbf{s}_2} \tag{22}$$

In addition, substituting Eq. (21) into Eq. (15) yields the matrix-vector form of $\boldsymbol{\varepsilon}_e$ as follows:

$$\boldsymbol{\varepsilon}_e = \boldsymbol{\varepsilon} - \mathbf{Q} \boldsymbol{\varepsilon} = \mathbf{P} \boldsymbol{\varepsilon} \tag{23}$$

where

$$\mathbf{P} = \mathbf{I} - \mathbf{Q} = \mathbf{I} - \frac{\mathbf{s}_2 \mathbf{s}_2^T \mathbf{C}}{\mathbf{s}_2^T \mathbf{C} \mathbf{s}_2} \tag{24}$$

and $\mathbf{I}$ is 3×3 identity matrix.

From Eqs. (21) and (23), the total strain vector $\boldsymbol{\varepsilon}$ can be expressed as

$$\boldsymbol{\varepsilon} = \boldsymbol{\varepsilon}_e + \boldsymbol{\varepsilon}_w = \mathbf{P} \boldsymbol{\varepsilon} + \mathbf{Q} \boldsymbol{\varepsilon} \tag{25}$$

In the preceding equation, the matrices $\mathbf{Q}$ and $\mathbf{P}$ are projection matrices that satisfy the following relations:

$$\mathbf{Q}^2 = \mathbf{Q}\mathbf{Q} = \frac{(\mathbf{s}_2^T \mathbf{C} \mathbf{s}_2) \mathbf{s}_2 \mathbf{s}_2^T \mathbf{C}}{(\mathbf{s}_2^T \mathbf{C} \mathbf{s}_2)(\mathbf{s}_2^T \mathbf{C} \mathbf{s}_2)} = \mathbf{Q} \tag{26}$$

$$\mathbf{P}^2 = \mathbf{P}\mathbf{P} = \mathbf{I} - 2\mathbf{Q} + \mathbf{Q}^2 = \mathbf{I} - \mathbf{Q} = \mathbf{P} \tag{27}$$

$$\mathbf{C}\mathbf{Q} = \frac{\mathbf{C} \mathbf{s}_2 \mathbf{s}_2^T \mathbf{C}}{\mathbf{s}_2^T \mathbf{C} \mathbf{s}_2} = (\mathbf{C}\mathbf{Q})^T \tag{28}$$

$$\mathbf{C}\mathbf{P} = \mathbf{C} - \mathbf{C}\mathbf{Q} = (\mathbf{C} - \mathbf{C}\mathbf{Q})^T = (\mathbf{C}\mathbf{P})^T \tag{29}$$

$$\mathbf{P}^T \mathbf{C}\mathbf{Q} = \mathbf{C}(\mathbf{I} - \mathbf{Q})\mathbf{Q} = \mathbf{0} \tag{30}$$

where $\mathbf{0}$ is 3×3 zero matrix. These relations are used in the next section.

Substituting Eq. (23) into Eq. (16) yields the stress–strain relations in the wrinkled membrane as

$$\boldsymbol{\sigma}_t = \mathbf{C}_m \boldsymbol{\varepsilon} \tag{31}$$

where $\mathbf{C}_m = \mathbf{C}\mathbf{P}$ is the modified elasticity matrix. The modified matrix is expressed as a product of the usual elasticity matrix and the projection matrix, and its physical understanding can be simply stated with reference to Fig. 3. The total strain vector $\boldsymbol{\varepsilon}$ is decomposed into the elastic strain vector $\boldsymbol{\varepsilon}_e$ and the wrinkle-mode deformation vector $\boldsymbol{\varepsilon}_w$ shown in the left-hand side of the figure. At first, the elastic strain vector $\boldsymbol{\varepsilon}_e$, shown in the middle of the figure, is obtained from $\boldsymbol{\varepsilon}$ by the projection matrix $\mathbf{P}$. Next, the uniaxial stress vector $\boldsymbol{\sigma}_t$, shown in the right-hand side of the figure, is mapped from $\boldsymbol{\varepsilon}_e$ by the usual elasticity matrix $\mathbf{C}$. Consequently, the modified elasticity matrix $\mathbf{C}_m$ is expressed as product of the usual elasticity matrix and the projection matrix.

Finally, we make some remarks on the wrinkle model described in this subsection.

Remark 1: By substituting $\theta = 0$ into the vectors $\mathbf{s}_1$ and $\mathbf{s}_2$ in Eqs. (6) and (18), we can express ε_{2w} in terms of the principal strains as follows:

$$\varepsilon_{2w} = \varepsilon_2 + \nu \varepsilon_1 \tag{32}$$

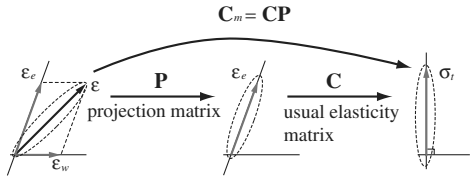

Fig. 3 Physical understanding of the modified elasticity matrix.

It should be noted that ε_{2w} becomes negative when we adopt the mixed stress–strain wrinkle criterion [20], in which the principal strains in a wrinkled state hold the following inequalities:

$$\varepsilon_1 > 0, \qquad \varepsilon_2 + \nu \varepsilon_1 < 0 \tag{33}$$

Remark 2: Premultiplying both sides of Eq. (25) by $\mathbf{C}$ yields the following stress decomposition:

$$\boldsymbol{\sigma} = \boldsymbol{\sigma}_t + \boldsymbol{\sigma}_w \tag{34}$$

where

$$\boldsymbol{\sigma}_t = \mathbf{C}\mathbf{P} \boldsymbol{\varepsilon} \tag{35}$$

$$\boldsymbol{\sigma}_w = \mathbf{C}\mathbf{Q} \boldsymbol{\varepsilon} \tag{36}$$

Further, by referring to Eqs. (2), (28), and (29), Eq. (34) can be rewritten by the transpose of the projection matrices as follows:

$$\boldsymbol{\sigma} = \mathbf{P}^T \boldsymbol{\sigma} + \mathbf{Q}^T \boldsymbol{\sigma} \tag{37}$$

Remark 3: From Eqs. (23), (30), and (36), we can find that the vectors $\boldsymbol{\varepsilon}_e$ and $\boldsymbol{\sigma}_w$ are orthogonal as follows:

$$\boldsymbol{\varepsilon}_e^T \boldsymbol{\sigma}_w = \boldsymbol{\varepsilon}^T \mathbf{P}^T \mathbf{C}\mathbf{Q} \boldsymbol{\varepsilon} = 0 \tag{38}$$

Remark 4: By substituting $\theta = 0$ into $\mathbf{Q}$ in Eq. (36), we obtain the components of $\boldsymbol{\sigma}_w$ in terms of the principal coordinate system as follows:

$$\boldsymbol{\sigma}_w = \begin{bmatrix} \nu \sigma_2 \\ \sigma_2 \\ 0 \end{bmatrix} \tag{39}$$

where

$$\sigma_2 = \frac{E}{1 - \nu^2} \varepsilon_{2w} \tag{40}$$

From Eqs. (33) and (40), we can observe that σ_2 becomes negative. This means that $\boldsymbol{\sigma}_w$ contains only compressive stress components that cannot be allowed in the TF theory.

Remark 5: By referring to Eq. (29), the stress–strain relations shown in Eq. (31) can be rewritten as

$$\boldsymbol{\sigma}_t = \mathbf{C}_m \boldsymbol{\varepsilon} = \mathbf{P}^T \mathbf{C} \boldsymbol{\varepsilon} \tag{41}$$

From the preceding equation, we can state another physical interpretation of the modified elasticity matrix with reference to Fig. 4. At first, the stress vector $\boldsymbol{\sigma}$ (which is decomposed into $\boldsymbol{\sigma}_t$ and $\boldsymbol{\sigma}_w$, as shown in the middle of the figure) is mapped from the total strain vector $\boldsymbol{\varepsilon}$ by the usual elasticity matrix $\mathbf{C}$. Next, the uniaxial

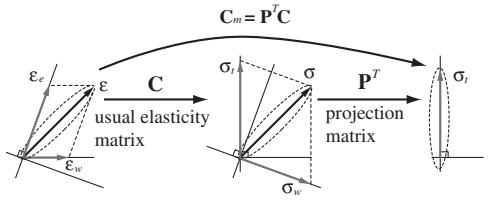

Fig. 4 Modified elasticity matrix based on the stress decomposition.

stress vector $\boldsymbol{\sigma}_t$, shown in the right-hand side of the figure, is obtained by the transpose of the projection matrix $\mathbf{P}$. Consequently, the modified elasticity matrix $\mathbf{C}_m$ is expressed as a product of $\mathbf{P}^T$ and $\mathbf{C}$.

Derivation of Sensitivity Analysis Method for Membrane Wrinkling

In this section, we derive a sensitivity analysis method for membrane wrinkling along with the wrinkle model presented in the preceding section. First, we introduce a quantifier that represents the intensity of membrane wrinkling. The quantifier is effectively defined by using the projection matrices given in the decomposition of the strain vectors. Next, we derive the sensitivity of the quantifier with respect to an arbitrary design parameter.

Wrinkle Intensity at a Material Point

We introduce a quantifier that represents the intensity of membrane wrinkling at a material point from the viewpoint of strain energy density. As described in the preceding section, the elastic deformation in a wrinkled membrane is represented by the elastic strain vector $\boldsymbol{\varepsilon}_e$. Therefore, the strain energy density at a material point in the wrinkled membrane can be expressed as follows:

$$\phi_e = \tfrac{1}{2}\boldsymbol{\varepsilon}_e^T \mathbf{C}\boldsymbol{\varepsilon}_e \tag{42}$$

By substituting Eq. (23) into Eq. (42) and referring to Eqs. (27) and (29), the strain energy density can also be represented by

$$\phi_e = \tfrac{1}{2}\boldsymbol{\varepsilon}^T \mathbf{P}^T \mathbf{C}\mathbf{P}\boldsymbol{\varepsilon} = \tfrac{1}{2}\boldsymbol{\varepsilon}^T \mathbf{C}\mathbf{P}\boldsymbol{\varepsilon} \tag{43}$$

Further, by substituting Eq. (24) into Eq. (43) and referring to Eqs. (21), (26), and (28), the strain energy density can be decomposed into the following two parts:

$$\phi_e = \tfrac{1}{2}\boldsymbol{\varepsilon}^T \mathbf{C}(\mathbf{I} - \mathbf{Q})\boldsymbol{\varepsilon} = \phi_p - \phi_w \tag{44}$$

where

$$\phi_p = \tfrac{1}{2}\boldsymbol{\varepsilon}^T \mathbf{C}\boldsymbol{\varepsilon} \tag{45}$$

$$\phi_w = \tfrac{1}{2}\boldsymbol{\varepsilon}_w^T \mathbf{C}\boldsymbol{\varepsilon}_w \tag{46}$$

Note that ϕ_p and ϕ_w are nonnegative scalar functions due to the positive definiteness of matrix $\mathbf{C}$. From Eq. (45), we can see that ϕ_p takes the same form as that of the usual membrane theory; that is, ϕ_p yields an actual elastic strain energy density when the stress state at a material point is the taut state, where $\phi_w = 0$. On the other hand, if the stress state is the wrinkled state, ϕ_p is overestimated when compared with the actual elastic strain energy density, because $\boldsymbol{\varepsilon}$ contains the wrinkle-mode deformation that produces no elastic energy. From Eq. (44), we can find that the excess energy contained in ϕ_p is indicated by ϕ_w. This excess energy can be considered as a quantifier of the intensity of membrane wrinkling because it depends on only the wrinkle-mode deformation $\boldsymbol{\varepsilon}_w$ shown in Eq. (46). Therefore, in this paper, we define ϕ_w as a quantifier that represents the intensity of membrane wrinkling at a material point.

Remark 6: By substituting $\theta = 0$ into the vector $\boldsymbol{\varepsilon}_w$ in Eq. (46), we can express ϕ_w in terms of the principal strains as follows:

$$\phi_w = \frac{E\varepsilon_{2w}^2}{2(1-\nu^2)} \tag{47}$$

This equation indicates that ϕ_w is a quadratic function of ε_{2w}.

Total Wrinkle Intensity over the Entire Membrane

Next, we introduce a quantifier that represents the total intensity of wrinkling over the entire membrane. Consider a membrane discretized by finite elements. In each element, we introduce a scalar function U_w^k in the integration form of ϕ_w as follows:

$$U_w^k \equiv \int_{V_e} \phi_w(r_1, r_2)\, \mathrm{d}V \tag{48}$$

where k denotes the element number, V_e denotes the volume of the undeformed membrane element, and r_i is the natural coordinate of the membrane element. The quantifier that represents the total intensity of wrinkling over the entire membrane is defined as a weighted summation of U_w^k by

$$U_w = \sum_{k=1}^{N_e} w^k U_w^k \tag{49}$$

where N_e denotes the total number of finite elements and w^k represents a weight coefficient of the kth element that is usually set to 1 and may be appropriately selected according to the design requirements.

Remark 7: In finite element calculations, U_w^k is obtained by performing Gauss numerical integration, in which the principal strains required for the calculation of ϕ_w in Eq. (47) are evaluated at each integration point. The total wrinkle intensity can be easily calculated as a weighted summation of U_w^k.

Sensitivity of ϕ_w with Respect to $\boldsymbol{\varepsilon}$

Here, we derive the sensitivity of ϕ_w with respect to the strain vector $\boldsymbol{\varepsilon}$. Referring to relations (26) and (28), Eq. (46) can be rewritten as

$$\phi_w = \tfrac{1}{2}\boldsymbol{\varepsilon}^T \mathbf{Q}^T \mathbf{C}\mathbf{Q}\boldsymbol{\varepsilon} = \tfrac{1}{2}\boldsymbol{\varepsilon}^T \mathbf{C}\mathbf{Q}\boldsymbol{\varepsilon} \tag{50}$$

Taking the time derivative of Eq. (50), we obtain

$$\dot{\phi}_w = \dot{\boldsymbol{\varepsilon}}^T \mathbf{C}\mathbf{Q}\boldsymbol{\varepsilon} + \tfrac{1}{2}\boldsymbol{\varepsilon}^T \mathbf{C}\dot{\mathbf{Q}}\boldsymbol{\varepsilon} \tag{51}$$

From Eq. (22), the time derivative of matrix $\mathbf{Q}$ is obtained as

$$\dot{\mathbf{Q}} = \frac{\dot{\mathbf{s}}_2\mathbf{s}_2^T\mathbf{C} + \mathbf{s}_2\dot{\mathbf{s}}_2^T\mathbf{C}}{\mathbf{s}_2^T\mathbf{C}\mathbf{s}_2} = -\frac{2(1-\nu^2)}{E}(\mathbf{n}_3\mathbf{s}_2^T\mathbf{C} + \mathbf{s}_2\mathbf{n}_3^T\mathbf{C})\dot{\theta} \tag{52}$$

In deriving the preceding equation, we use the following relations:

$$\mathbf{s}_2^T\mathbf{C}\mathbf{s}_2 = \frac{E}{1-\nu^2} = \text{const}, \qquad \dot{\mathbf{s}}_2 = -2\mathbf{n}_3\dot{\theta} \tag{53}$$

Substituting Eq. (52) into the second term in the right-hand side of Eq. (51) and referring to the equation $f(\theta) = \mathbf{n}_3^T\mathbf{C}\boldsymbol{\varepsilon} = 0$ shown in Eq. (10) yields

$$\frac{1}{2}\boldsymbol{\varepsilon}^T\mathbf{C}\dot{\mathbf{Q}}\boldsymbol{\varepsilon} = \frac{(1-\nu^2)}{E}[(\mathbf{n}_3^T\mathbf{C}\boldsymbol{\varepsilon})^T\mathbf{s}_2^T\mathbf{C}\boldsymbol{\varepsilon} + \boldsymbol{\varepsilon}^T\mathbf{C}\mathbf{s}_2(\mathbf{n}_3^T\mathbf{C}\boldsymbol{\varepsilon})]\dot{\theta} = 0 \tag{54}$$

Hence, substituting Eq. (54) into Eq. (51), we obtain the sensitivity of ϕ_w with respect to $\boldsymbol{\varepsilon}$ as follows:

$$\frac{\partial\phi_w}{\partial\boldsymbol{\varepsilon}} = \mathbf{C}\mathbf{Q}\boldsymbol{\varepsilon} \tag{55}$$

Remark 8: From Eqs. (36) and (55), we can find that ϕ_w corresponds to a potential function that produces the compressive stress vector $\boldsymbol{\sigma}_w$.

Sensitivity of U_w with Respect to the Design Parameter

Differentiating Eq. (48) with respect to the nodal displacement vector of the kth element $\mathbf{u}_e^k$, we obtain

$$\frac{\partial U_w^k}{\partial\mathbf{u}_e^k} = \int_{V_e} \mathbf{B}_L^{kT}\frac{\partial\phi_w}{\partial\boldsymbol{\varepsilon}}\, \mathrm{d}V \tag{56}$$

where

$$\mathbf{B}_L^k = \frac{\partial\boldsymbol{\varepsilon}}{\partial\mathbf{u}_e^k} \tag{57}$$

is the usual strain-displacement relation matrix. Substituting Eq. (55) into Eq. (56) yields the sensitivity of U_w^k with respect to $\mathbf{u}_e^k$ as follows:

$$\frac{\partial U_w^k}{\partial \mathbf{u}_e^k} = \int_{V_e} \mathbf{B}_L^{k^T} \mathbf{C}\mathbf{Q}\boldsymbol{\varepsilon}\, \mathrm{d}V \tag{58}$$

Now, let $\mathbf{u}_g$ be the global displacement vector given by

$$\mathbf{u}_e^k = \mathbf{L}^k \mathbf{u}_g \tag{59}$$

where $\mathbf{L}^k$ is the Boolean matrix that represents the relation between the global degree of freedom and the local one in the kth element. From Eqs. (49), (58), and (59), we obtain the sensitivity of U_w with respect to $\mathbf{u}_g$ as

$$\frac{\partial U_w}{\partial \mathbf{u}_g} = \sum_{k=1}^{N_e} w^k \mathbf{L}^{k^T} \frac{\partial U_w^k}{\partial \mathbf{u}_e} \tag{60}$$

The sensitivity of U_w with respect to an arbitrary design parameter can be effectively obtained by the SDM [13,14]. Now let $\mathbf{q}$ be the internal force vector. Then the equilibrium equation in the nonlinear finite element method can be written as

$$\mathbf{q}\,(\mathbf{u}_g(b_j), b_j) = \mathbf{f} \tag{61}$$

where b_j is the jth design parameter and $\mathbf{f}$ is the external force vector. Considering the variation of b_j, the variational form of Eq. (61) is given by

$$\frac{\partial \mathbf{q}}{\partial \mathbf{u}_g}\delta \mathbf{u}_g + \frac{\partial \mathbf{q}}{\partial b_j}\delta b_j = \mathbf{0} \tag{62}$$

From the preceding equation, the sensitivity of $\mathbf{u}_g$ is given by

$$\frac{\mathrm{d}\mathbf{u}_g}{\mathrm{d}b_j} = -\mathbf{K}^{-1}\frac{\partial \mathbf{q}}{\partial b_j} \tag{63}$$

where

$$\mathbf{K} = \frac{\partial \mathbf{q}}{\partial \mathbf{u}_g} \tag{64}$$

is the tangent stiffness matrix in the equilibrium state. In the SDM, the sensitivity of $\mathbf{q}$ is approximated by numerical differentiation as

$$\frac{\partial \mathbf{q}}{\partial b_j} \simeq \frac{\Delta \mathbf{q}}{\Delta b_j} \tag{65}$$

where Δb_j is a minute perturbation that is assumed numerically and $\Delta \mathbf{q}$ is a variation of $\mathbf{q}$ according to the minute perturbation. Therefore, from Eqs. (60), (63), and (65), we obtain the sensitivity of U_w with respect to an arbitrary design parameter as

$$\frac{\mathrm{d}U_w}{\mathrm{d}b_j} = \frac{\partial U_w}{\partial \mathbf{u}_g}\frac{\mathrm{d}\mathbf{u}_g}{\mathrm{d}b_j} \simeq \left(-\mathbf{K}^{-1}\frac{\Delta \mathbf{q}}{\Delta b_j}\right)^T \sum_{k=1}^{N_e} w^k \mathbf{L}^{k^T}\frac{\partial U_w^k}{\partial \mathbf{u}_e} \tag{66}$$

In practice, matrix $\mathbf{K}$ has already factored in the calculation of the Newton–Raphson method to search the equilibrium state, and therefore the calculation of $\mathbf{K}^{-1}\Delta \mathbf{q}/\Delta b_j$ can be easily performed by substitution. The numerical calculation of Eq. (60) is simply performed in the same way as that of the internal force vector. Therefore, the calculation of Eq. (66) can be easily performed in conjunction with usual nonlinear finite element analysis codes.

Remark 9: The sensitivity of U_w can be numerically evaluated by the direct differentiation method (DDM) [14] as follows:

$$\mathrm{d}\,U_w/\mathrm{d}b_j \simeq \Delta U_w/\Delta b_j \tag{67}$$

where ΔU_w is a variation of U_w according to the minute perturbation Δb_j. In this method, full nonlinear finite element analysis must be repeatedly performed in accordance with the number of design parameters. Therefore, this method is not practical for large-scale problems, although it is simple and accurate.

Wrinkle-Reduction Design by Sensitivity Analysis

In this section, we apply the sensitivity analysis method presented in the preceding section to the wrinkle-reduction design of membrane structures using a simple line-search method.

One-Dimensional Minimization Problem of U_w

Let N_d be the number of design parameters and we define the design parameter vector as

$$\mathbf{b} = [\,b_1 \quad \cdots \quad b_{N_d}\,]^T \tag{68}$$

Then the sensitivity vector of $U_w(\mathbf{b})$ is given as follows:

$$\mathrm{d}\,U_w/\mathrm{d}\mathbf{b} = [\,\mathrm{d}U_w/\mathrm{d}b_1 \quad \cdots \quad \mathrm{d}U_w/\mathrm{d}b_{N_d}\,]^T \tag{69}$$

It should be noted that the vector $-\mathrm{d}U_w/\mathrm{d}\mathbf{b}$ indicates the steepest-descent direction of $U_w(\mathbf{b})$ with respect to $\mathbf{b}$. To design membrane structures that would reduce the occurrence of wrinkles, we have to determine the appropriate design parameters to reduce $U_w(\mathbf{b})$. Therefore, we introduce the following one-dimensional minimization problem of $U_w(\mathbf{b})$ with respect to the step variable s for the wrinkle-reduction design:

Minimize:

$$U_w\left(\mathbf{b} - s\left.\frac{\mathrm{d}U_w}{\mathrm{d}\mathbf{b}}\right|_{\mathbf{b}=\mathbf{b}^{(0)}}\right) \tag{70}$$

where $\mathbf{b}^{(0)}$ is an initial design parameter vector, and the sensitivity vector is normalized as

$$\left|\frac{\mathrm{d}U_w}{\mathrm{d}\mathbf{b}}\right| = 1 \tag{71}$$

This minimization problem can be resolved by a simple incremental line search as follows:

$$\mathbf{b}^{(i+1)} = \mathbf{b}^{(0)} - s^{(i)}\left.\frac{\mathrm{d}U_w}{\mathrm{d}\mathbf{b}}\right|_{\mathbf{b}=\mathbf{b}^{(0)}} \tag{72}$$

$$s^{(i+1)} = s^{(i)} + a_c \tag{73}$$

where i is the step number of the line search and a_c is a small constant value. The initial value of $s^{(i)}$ is set to 0. It should be noted that $\mathbf{b}^{(i)}$ in Eq. (72) linearly increases with the step number i because the sensitivity vector is unchanging, whereas s linearly increases with the step number. The line search is continued until the following condition holds true:

$$U_w(\mathbf{b}^{(i+1)}) \geq U_w(\mathbf{b}^{(i)}) \tag{74}$$

The solution procedure for the one-dimensional optimization problem is briefly illustrated in Fig. 5. First, we set the initial design parameters. Next, the nonlinear finite element analysis is performed based on the TF theory to determine the equilibrium state, during which the objective function shown in Eq. (70) is calculated. Further, if the step number i is equal to 0, the sensitivity vector is calculated by employing Eq. (69). If the condition in Eq. (74) holds true, the optimization process is completed. Otherwise, the step value and the design parameters are updated by using Eqs. (72) and (73), respectively, and the line search continues. In the following subsections, some numerical examples will be shown to demonstrate the effectiveness of the proposed sensitivity analysis method. In these examples, the preceding solution procedure is implemented in the finite element analysis code developed by the authors, in which the modifications to the design parameters are performed automatically.

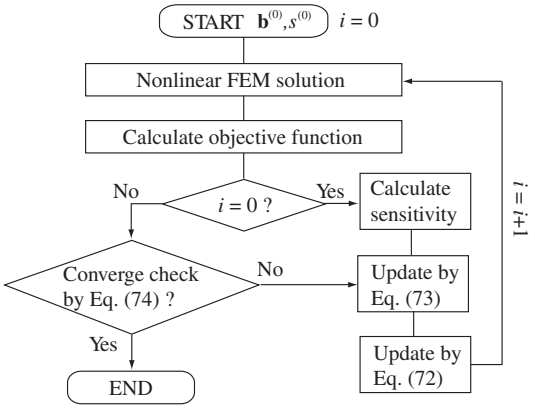

Fig. 5 Flowchart in the one-dimensional optimization problem.

Example 1: Cable Design Problem

Consider a square membrane supported by a rigid frame via tie cables at the corners, in which significant wrinkles appear. We attempt to reduce these wrinkles by setting two design cables near the corners. The design model for this problem is shown in Fig. 6. By symmetry, only the right half of the structure is modeled. The support frame size is chosen as 3.6 m. The membrane, for which the size and thickness are 3.5 m and 100 μm, respectively, is discretized using 14×14 nine-node membrane elements. All the nodes along the left edge are fixed in the x direction and all the nodes along the lower edge are fixed in the y direction. Poisson's ratio and Young's modulus of the membrane are given as $\nu = 0.33$ and $E = 480$ MPa, respectively. The tie cable and design cables, for which the axial stiffness values are $E_c A = 110$ MN, are modeled by using the two-node cable element that can sustain only tensile stresses. The natural length of the tie cable is set to 140 mm. The first design cables are set on both free edges at 1.5 m from the corner. The second design cables are set on both free edges at 0.5 m from the corner. The natural lengths of the first and second design cables are considered as the design parameters b_1 and b_2, respectively. The initial values of design parameters are chosen as $b_1^{(0)} = 99.8$ mm and $b_2^{(0)} = 99.7$ mm.

At first, we conduct the nonlinear finite element analysis based on the TF theory [12] to determine the equilibrium state of the membrane structure in the initial design parameters. Subsequently, the sensitivities are calculated by the formula presented in Eq. (66). The weight coefficient of all elements is set to $w^k = 1$. In this example, the numerical differentiation in Eq. (65) is performed by the backward difference, as shown next:

$$\frac{\Delta \mathbf{q}}{\Delta b_j} = \frac{\mathbf{q}(b_j) - \mathbf{q}(b_j - \Delta b_j)}{\beta b_j} \tag{75}$$

where β is a minute perturbation. To verify the accuracy of the sensitivities obtained by the proposed method, they are also calculated by using the DDM with the backward difference as follows:

$$\frac{\mathrm{d}U_w}{\mathrm{d}b_j} \simeq \frac{U_w(b_j) - U_w(b_j - \Delta b_j)}{\beta b_j} \tag{76}$$

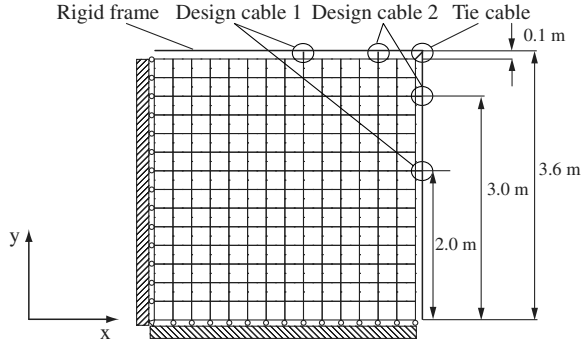

Fig. 6 Cable design model.

Table 1 Comparison of DDM and the proposed method for example 1

	DDM		Proposed	
β	$\mathrm{d}U_w/\mathrm{d}b_1$	$\mathrm{d}U_w/\mathrm{d}b_2$	$\mathrm{d}U_w/\mathrm{d}b_1$	$\mathrm{d}U_w/\mathrm{d}b_2$
1.0×10^{-5}	-0.45017×10^{-1}	0.99899	-0.44538×10^{-1}	0.99901
1.0×10^{-6}	-0.44586×10^{-1}	0.99901	-0.44538×10^{-1}	0.99901
1.0×10^{-7}	-0.44543×10^{-1}	0.99901	-0.44538×10^{-1}	0.99901
1.0×10^{-8}	-0.44539×10^{-1}	0.99901	-0.44539×10^{-1}	0.99901
1.0×10^{-9}	-0.44543×10^{-1}	0.99901	-0.44546×10^{-1}	0.99901

Table 1 shows the comparison of sensitivities calculated by using the DDM and the proposed method. The value of β is chosen from the range of 1.0×10^{-5}–1.0×10^{-9}. As shown in the table, the sensitivities calculated by both methods are in very good agreement to three or more significant digits with each other except $\beta = 1.0 \times 10^{-5}$, which indicates the accuracy of the proposed calculation scheme. From these sensitivities, we can observe that design cable 2 has more significant effect on U_w than design cable 1.

Next, we perform an incremental line search according to Eqs. (72) and (73). The value of β required for the calculation of $\partial U_w/\partial b_j$ is set to 1.0×10^{-6}. The constant value a_c is set to 2.0×10^{-5}. Figure 7 shows the variations in the normalized objective function $\bar{U}_w$, which is the ratio of $U_w(\mathbf{b}^{(i)})$ to $U_w(\mathbf{b}^{(0)})$. In this problem, the line search stopped at the 12th step. As observed, $\bar{U}_w$ monotonically decreases and, in the last step, reduces to 22% of the initial design. The variations in the normalized design parameters $\bar{b}_j$, which is the ratio of $b_j^{(i)}$ to $b_j^{(0)}$, are shown in Fig. 8. From this figure, we can observe that the natural length of the cable b_2 is decreased, whereas b_1 is almost unchanged. The directions of wrinkles in the first and last steps are depicted in Fig. 9. The wrinkle directions are expressed as straight lines for which the lengths are uniformly identical to those of each element. From this figure, we can observe that the wrinkled regions around the corner are considerably reduced in the design parameters of the last step.

Example 2: Thickness Design Problem

We consider the thickness design problem of a square membrane tensioned by forced displacements at the corners. The design model for this problem is depicted in Fig. 10. By symmetry, only the right half of the membrane is modeled and discretized using 20×20 nine-node membrane elements. All the nodes along the left edge are fixed in the x direction and all the nodes along the lower edge are fixed in the y direction. The membrane size and thickness are 1.0 m and 100 μm, respectively. Poisson's ratio and Young's modulus of the membrane are given as $\nu = 0.33$ and $E = 480$ MPa, respectively. The forced displacement at the corner is set to 5.0 mm. The elements on both free edges are equally divided among four groups, and the thicknesses in each group are defined as the design parameters

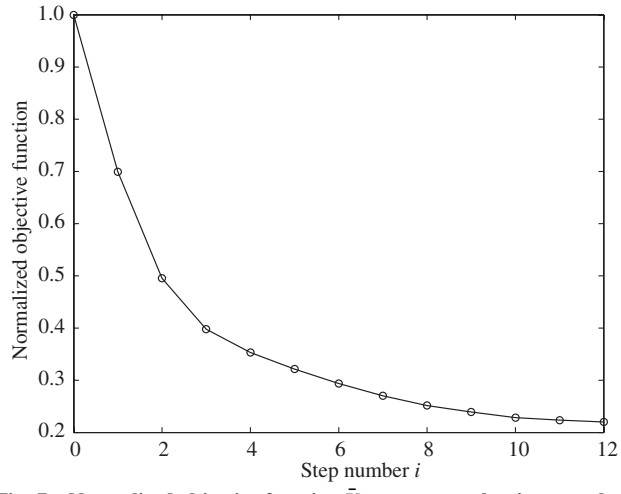

Fig. 7 Normalized objective function $\bar{U}_w$ vs step number in example 1.

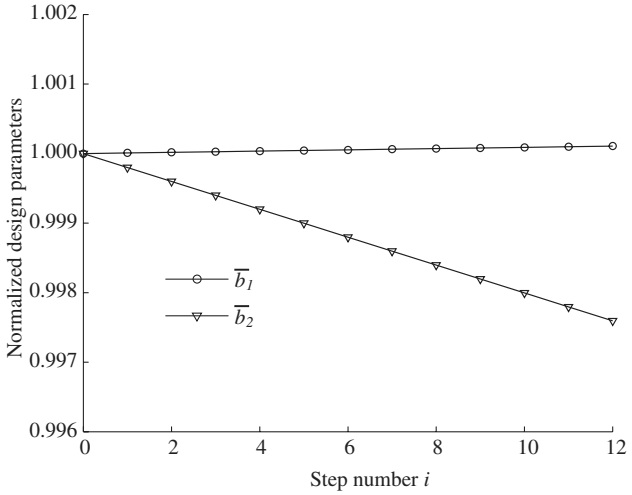

Fig. 8 Variations in the design parameters in example 1.

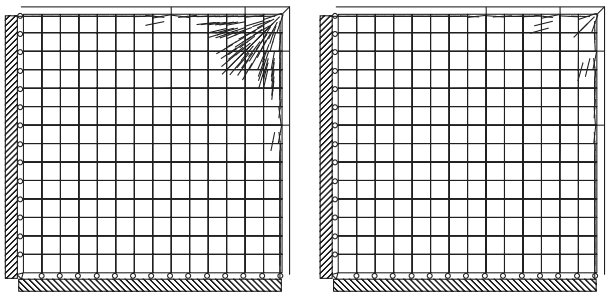

a) Step 0, $\overline{U}_w = 1.00$ **b) Step 12, $\overline{U}_w = 0.22$**

Fig. 9 Directions of wrinkles in example 1.

$b_j (j = 1 \sim 4)$. The initial values of all the design parameters are chosen as $b_j^{(0)} = 500\ \mu$m.

First, we conduct the nonlinear finite element analysis based on the TF theory using the initial design parameters and calculate the sensitivities by employing the DDM and the proposed method. The weight coefficient of all elements is set to $w^k = 1$. In this example, the numerical differentiations in both methods are performed by the central differences, as shown next.

$$\frac{\Delta \mathbf{q}}{\Delta b_j} = \frac{\mathbf{q}(b_j + \Delta b_j) - \mathbf{q}(b_j - \Delta b_j)}{2\beta b_j} \tag{77}$$

$$\frac{\mathrm{d}U_w}{\mathrm{d}b_j} \simeq \frac{U_w(b_j + \Delta b_j) - U_w(b_j - \Delta b_j)}{2\beta b_j} \tag{78}$$

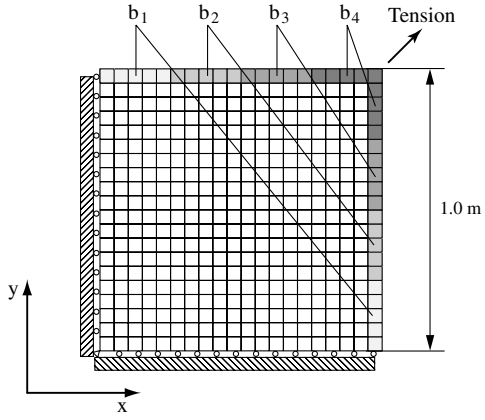

Fig. 10 Thickness design model.

Table 2 Comparison of DDM and the proposed method for example 2

β	$\partial U_w/\partial b_1$	$\partial U_w/\partial b_2$	$\partial U_w/\partial b_3$	$\partial U_w/\partial b_4$
		DDM		
1.0×10^{-5}	−0.71815	-0.29890×10^{-1}	0.40836	0.56268
1.0×10^{-6}	−0.71815	-0.29890×10^{-1}	0.40836	0.56268
1.0×10^{-7}	−0.71815	-0.29888×10^{-1}	0.40836	0.56268
1.0×10^{-8}	−0.71814	-0.29901×10^{-1}	0.40837	0.56268
1.0×10^{-9}	−0.71807	-0.30082×10^{-1}	0.40848	0.56268
		Proposed		
1.0×10^{-5}	−0.72824	-0.29985×10^{-1}	0.40785	0.54993
1.0×10^{-6}	−0.72824	-0.29985×10^{-1}	0.40785	0.54993
1.0×10^{-7}	−0.72824	-0.29985×10^{-1}	0.40785	0.54993
1.0×10^{-8}	−0.72824	-0.29985×10^{-1}	0.40785	0.54993
1.0×10^{-9}	−0.72824	-0.29985×10^{-1}	0.40785	0.54993

Table 2 shows the comparison of sensitivities calculated by both methods in which the value β is chosen from the range of 1.0×10^{-5}–1.0×10^{-9}. As shown in the table, a good agreement is found between both methods, although the small constant differences are found. These differences may be reduced by refining the finite element mesh of the membrane.

Next, we conduct an incremental line search to reduce the wrinkles on the membrane. The sensitivity vector is evaluated by the proposed method, in which the values β and a_c are set to 1.0×10^{-6} and 2.0×10^{-5}, respectively. The variations in the normalized objective function in each step are illustrated in Fig. 11. The line search is stopped at the 26th step. We can observed that, similar to example 1, $\bar{U}_w$ decreases monotonically. In the last step, $\bar{U}_w$ decreases to 0.012% of the initial design. Figure 12 indicates the variations in the normalized design parameters. It is observed that the thicknesses of two groups near the corner decrease, whereas those of the other two groups increase. Figure 13 shows the directions of wrinkles, which are expressed as straight lines, in the first and last steps. In this figure, the design parameters are also depicted in linear grayscale. From the figure, we can observe that the wrinkled regions are considerably reduced in the last step.

Shape Optimization of the Square Membrane for Wrinkle-Reduction Design

In this section, we consider the shape optimization problem of a square membrane for the wrinkle-reduction design. The optimization is performed by the exterior penalty function method [46] and the proposed sensitivity analysis method.

Design Model

Consider a membrane tensioned at each corner by forced displacements. In the membrane, wrinkles appear around the corners

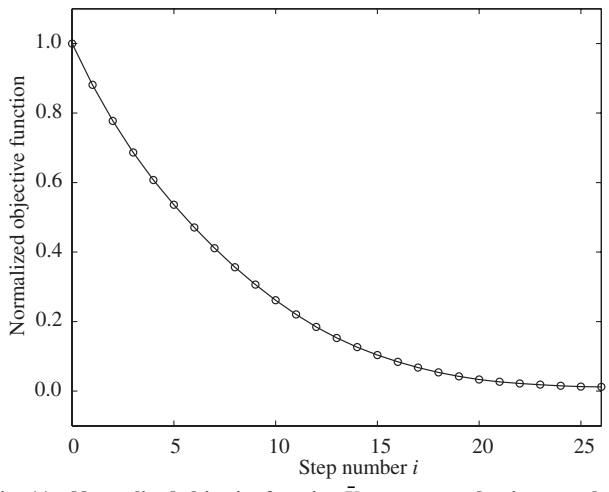

Fig. 11 Normalized objective function $\bar{U}_w$ vs step number in example 2.

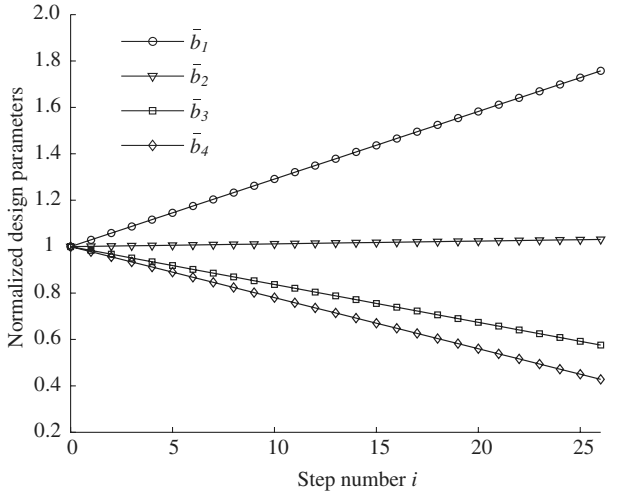

Fig. 12 Variations in the design parameters in example 2.

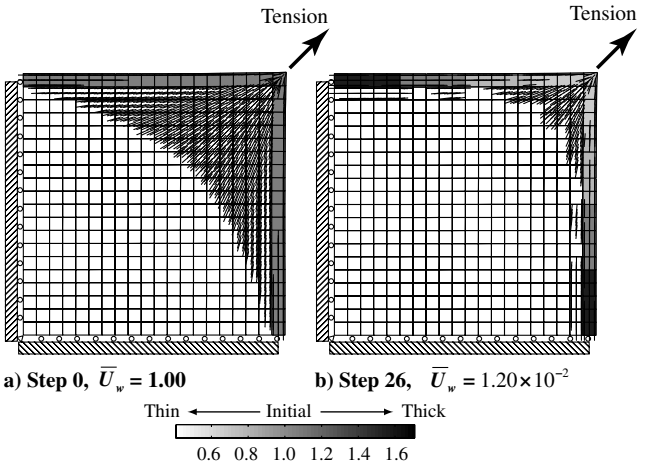

Fig. 13 Directions of wrinkles in example 2.

and the edges [47,48]. To reduce those wrinkles, the edge shapes of the membrane are designed by an optimization method. The design model is shown in Fig. 14, in which the membrane is modeled as a quarter-square triangle by considering the symmetry. For the edge-shape design, the hypotenuse of the triangle is bent according to the design parameters b_1 and b_2, which denote the normal distance from the bending point to the lower leg and the distance between the midpoint of the hypotenuse and the vertex of the right angle of the membrane, respectively. The bent line is defined to be symmetric to the perpendicular bisector of the hypotenuse. It is assumed that the membrane is made of polyimide film with a thickness $t = 50$ μm. The size of the membrane is chosen as 1.0 m. Poisson's ratio and Young's modulus are given as $\nu = 0.34$ and $E = 2.96$ GPa, respectively.

A finite element model for this problem is shown in Fig. 15. The model is discretized by 4500 four-node membrane elements. All the nodes along the left edge are fixed in the x direction and all the nodes along the lower edge are fixed in the y direction. To avoid severe mesh distortion, the sharp corners of the membrane are truncated by the lines with a length d$s = 10$ mm. These lines are divided into 30 elements and displaced by 5.0 mm. Figure 15 also describes the distribution of the weight coefficient w^k. In this example, we aim to reduce the wrinkles near the central region of the membrane, and thus the weight coefficients of the elements along the hypotenuse and around the sharp corners (three elements from the truncated line), in which the wrinkles are significantly large but have less effect on the design, are set to $w^k = 0$ for efficiency. The weight coefficient of other elements is set to $w^k = 1$.

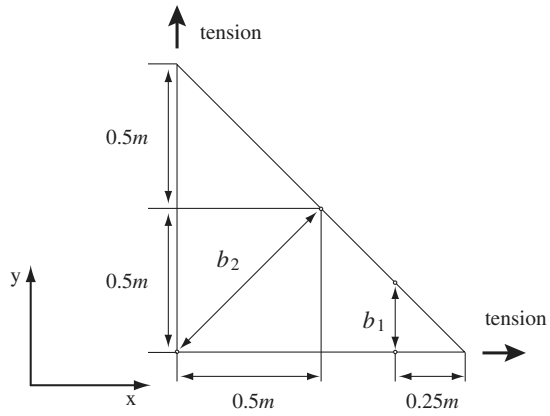

Fig. 14 Shape design model.

Optimization Problem

The objective of the shape optimization problem for the wrinkle-reduction design is to reduce U_w, whereas the membrane area may also be an important design factor in the practical design. Therefore, we consider the following constrained minimization problem:

Minimize:

$$U_w(\mathbf{b}) \tag{79a}$$

Subject to:

$$S(\mathbf{b}) \geq \gamma S_0 \tag{79b}$$

where $S(\mathbf{b})$ and S_0 denote the designed membrane area and the initial membrane area, respectively, and γ indicates the minimum value of the ratio of the required membrane area to S_0. This problem can be replaced by the unconstrained minimization problem by using the exterior penalty function method [46], as shown next.

Minimize:

$$\varphi(\mathbf{b}) \tag{80}$$

$$\varphi(\mathbf{b}) = U_w(\mathbf{b}) + rU_s(\mathbf{b}) \tag{81}$$

where $U_s(\mathbf{b})$ is the penalty function for the area constraint given by

$$U_s(\mathbf{b}) = \min[0, (S(\mathbf{b}) - \gamma S_0)]^2 \tag{82}$$

and r is the penalty coefficient. This problem can be resolved by the steepest-descent method. In the lth iteration step of the steepest-descent method, the design parameter vector is updated as follows, according to the same incremental line search used in the preceding section:

$$\mathbf{b}_l^{(i+1)} = \mathbf{b}_l^{(0)} - s^{(i+1)} \frac{\mathrm{d}\varphi}{\mathrm{d}\mathbf{b}}\bigg|_{\mathbf{b}=\mathbf{b}_l^{(0)}} \tag{83}$$

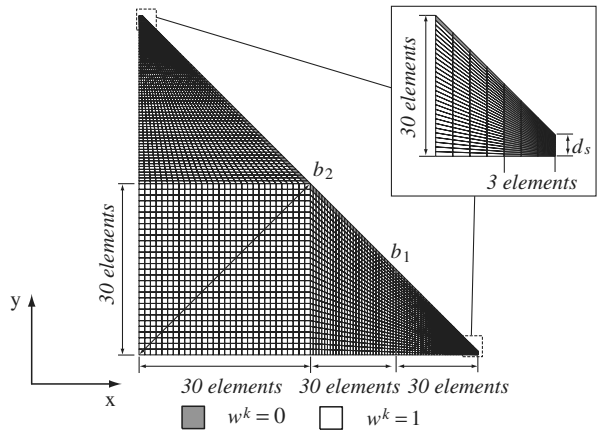

Fig. 15 Finite element mesh and weight coefficients.

$$s^{(i+1)} = s^{(i)} + a_c \tag{84}$$

$$\frac{\mathrm{d}\varphi}{\mathrm{d}\mathbf{b}} = \left[\frac{\mathrm{d}U_w}{\mathrm{d}b_1} + r\frac{\mathrm{d}U_s}{\mathrm{d}b_1}\ \frac{\mathrm{d}U_w}{\mathrm{d}b_2} + r\frac{\mathrm{d}U_s}{\mathrm{d}b_2}\right]^T \tag{85}$$

where the sensitivity vector $\mathrm{d}\varphi/\mathrm{d}\mathbf{b}$ is calculated in the first step of the line search at each iteration. The step number i is incremented until the same condition as in Eq. (74) holds as

$$\varphi(\mathbf{b}_l^{(i+1)}) \geq \varphi(\mathbf{b}_l^{(i)}) \tag{86}$$

At the last step of the line search ($i = n_l$), the design parameter vector is updated as

$$\mathbf{b}_{l+1}^{(0)} = \mathbf{b}_l^{(n_l)} \tag{87}$$

Then the new sensitivity vector is calculated based on $\mathbf{b}_{l+1}^{(0)}$. The optimization process continues until the following condition holds true:

$$\varphi(\mathbf{b}_{l+1}^{(n_l)}) \geq \varphi(\mathbf{b}_l^{(n_l)}) \tag{88}$$

Figure 16 summarizes the solution procedure for the presented shape optimization problem. At first, we set the initial design parameters to define the initial shape of the membrane. Further, the nonlinear finite element analysis is performed based on the TF theory to determine the equilibrium state, during which the objective function shown in Eq. (81) is calculated. Further, if the line-search step number i is equal to 0, the sensitivity vector is calculated by employing Eq. (85). Unless the condition in Eq. (86) holds true, the step value and the design parameters are updated by using Eqs. (83) and (84). If the condition in Eq. (88) holds true, the optimization process is completed. This solution procedure is implemented in the finite element analysis code developed by the authors.

Results

The shape optimization is performed for $\gamma = 0.85$, which means that the lower limit area of the optimized membrane is constrained to 0.85 times the area of the initial membrane. The values of r and a_c are chosen as 1.0×10^3 and 1.0×10^{-3}, respectively. The sensitivity vector $\mathrm{d}U_w/\mathrm{d}\mathbf{b}$ is evaluated by the proposed formula shown in Eq. (66), in which the central difference is used with $\beta = 1.0 \times 10^{-6}$ to perform the numerical differentiation. Figure 17 shows the convergence behaviors of the optimization process. In the figure, only the values at $i = 0$ are plotted, for simplicity. As can be seen, both design parameters gradually decrease and converge at the 22nd iteration step. The normalized objective function $\bar{\varphi}$, which is defined as the ratio of $\varphi(\mathbf{b}_l^{(0)})$ to $\varphi(\mathbf{b}_0^{(0)})$, reduces to 23% of the initial design in the final step. The area ratio $\bar{S}$ defined by the ratio of $S(\mathbf{b}_l^{(0)})$ to S_0

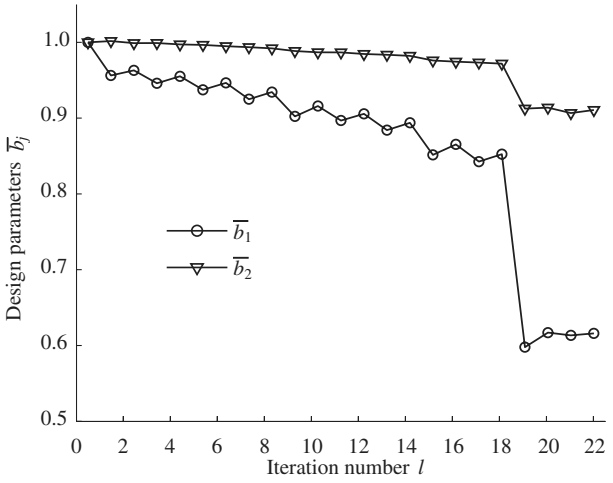

a) Variations of design parameters

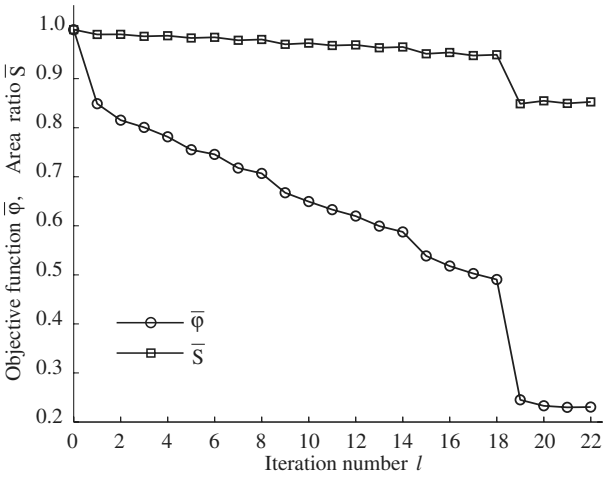

b) Variations of objective function and area ratio

Fig. 17 Convergence behaviors of the optimization process.

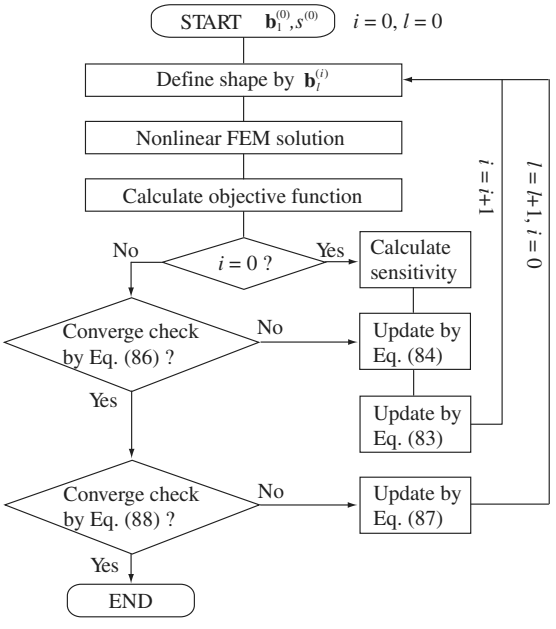

Fig. 16 Flowchart in the shape optimization process.

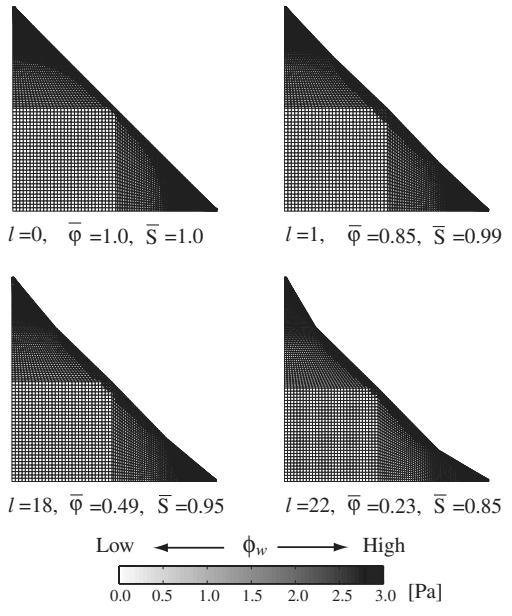

Fig. 18 Designed shapes and distributions of ϕ_w.

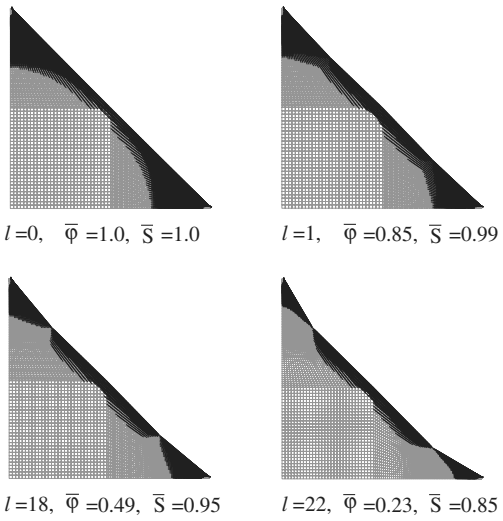

Fig. 19 Directions of wrinkles in example 3.

converges to 0.85, which indicates that the optimized solution satisfies the area constraint corresponding to $\gamma = 0.85$. The obtained shapes and distributions of ϕ_w at $l = 0$, 1, 18, and 22 are shown in Fig. 18. In this figure, the distributions are illustrated by interpolating ϕ_w at each node, and all the values greater than 3.0 Pa are rounded to 3.0 Pa for display. The directions of wrinkles are also depicted in Fig. 19. From these figures, it can be observed that there are large wrinkled regions around the sharp corners and along the edge in the initial design ($l = 0$). After the first iteration step ($l = 1$), $\bar{\varphi}$ reduces to 85% of the initial design and the wrinkled regions decrease (mainly near the sharp corners), whereas the shape of the membrane is almost unchanged. With increasing iteration steps ($l = 18, 22$), the wrinkled regions around the sharp corners gradually reduce, thereby leading to a decrease in the sharp corner angles.

Conclusions

A new sensitivity analysis method for membrane wrinkling is presented based on the tension-field theory. In the present method, the formulas to evaluate both the total intensity of wrinkling over the entire membrane and its sensitivity with respect to an arbitrary design parameter are developed. The method is applied to some examples in which the minimization problems for the total intensity of membrane wrinkling are resolved to obtain wrinkle-reduction designs. The results reveal the accuracy and effectiveness of the proposed method. The proposed method can cope with a wider class of optimization problems for the reduction in membrane wrinkling.

Acknowledgments

The authors thank Kyoichi Nakashino, Tokai University, Japan, for his helpful comments and discussions.

References

[1] Lin, J. K., Sapna, G. H., III, and Scarborough S. E., "Advanced Precipitation Radar Antenna Singly Curved Parabolic Antenna Reflector Development," AIAA Paper 2003-1651, Apr. .2003.

[2] Talley, C., Clayton, W., Gierow, P., Laue, G., McGee, J., and Moore, J., "Advanced Membrane Materials for Improved Solar Sail Capabilities," AIAA Paper 2002-1561, Apr. .2002.

[3] Otto, F., and Rasch, B., *Finding Form: Towards an Architecture of the Minimal*, 1st ed., Edition Axel Menges, Stuttgart, 1995.

[4] Bletzinger, K. U., and Ramm, E., "Structural Optimization and Form Finding of Light Weight Structures," *Computers and Structures*, Vol. 79, Nos. 22–25, 2001, pp. 2053–2062. doi:10.1016/S0045-7949(01)00052-9

[5] Mikulas, M. M., and Adler, A. L., "Rapid Structural Assessment Approach for Square Solar Sails Including Edge Support Cords," AIAA Paper 2003-1447, Apr. 2003.

[6] Greschik, G., White, C. V., and Salama, M. A., "On the Precisely Uniform and Uniaxial Tensioning of a Film Sheet via Integrated Catenary," AIAA Paper 2003-1906, Apr. 2003.

[7] Sakamoto, H., Park, K. C., and Miyazaki, Y., "Dynamic Wrinkle Reduction Strategies for Cable-Suspended Membrane Structures," *Journal of Spacecraft and Rockets*, Vol. 42, No. 5, 2005, pp. 850–858. doi:10.2514/1.11328

[8] Leifer, J., "Simplified Computational Models for Shear-Compliant Borders in Solar Sails," *Journal of Spacecraft and Rockets*, Vol. 44, No. 3, 2007, pp. 571–581. doi:10.2514/1.20907

[9] Johnston, J. D., "Finite Element Analysis of Wrinkled Membrane Structures for Sunshield Applications," AIAA Paper 2002-1456, Apr. 2002.

[10] Murphey, T. W., Murphy, D. M., Mikulas, M. M., and Adler, A. L., "A Method to Quantify the Thrust Degradation Effects of Structural Wrinkles in Solar Sails," AIAA Paper 2002-1560, Apr. 2002.

[11] Akita, T., Nakashino, K., Natori, M. C., and Park, K. C., "Derivation of Modified Stress–Strain Tensor for Wrinkled Membrane by Using Projection Matrix," *Computational Mechanics (WCCM 6)* [CD-ROM], Tsinghua Univ. Press, Beijing, and Springer–Verlag, New York, 2004.

[12] Akita, T., Nakashino, K., Natori, M. C., and Park, K. C., "A Simple Computer Implementation of Membrane Wrinkle Behaviour via a Projection Technique," *International Journal for Numerical Methods in Engineering*, Vol. 71, No. 10, 2007, pp. 1231–1259. doi:10.1002/nme.1990

[13] Hisada, T., "Sensitivity Analysis of Nonlinear FEM," *Probabilistic Methods in Civil Engineering*, American Society of Civil Engineers, New York, 1988, pp. 160–163.

[14] Chen, X., Hisada, T., Kleiber, M., and Noguchi, H., "Comparison of Different Sensitivity Analysis Algorithms for Large Deformation Elastic-Plastic Problems," *Design-Sensitivity Analysis*, Atlanta Technology Publications, Atlanta, 1993, pp. 209–229.

[15] Wagner, H., "Ebene Blechwandtrager mit sehr Dunnem Stegblech," *Zeitschrift für Flugtechnik und Motorluftschiffahrt*, Vol. 20, 1929, pp. 200–314.

[16] Libai, A., and Simmonds, J. G., *The Nonlinear Theory of Elastic Shells*, 2nd ed., Cambridge Univ. Press, New York, 1998, pp. 276–280, 431–441.

[17] Miller, R. K., Hedgepeth, J. M., Weingarten, VI., Das, P., and Kahyai, S., "Finite Element Analysis of Partly Wrinkled Membranes," *Computers and Structures*, Vol. 20, Nos. 1–3, 1985, pp. 631–639. doi:10.1016/0045-7949(85)90111-7

[18] Adler, A. L., and Mikulas, M. M., "Application of a Wrinkled Membrane Finite Element Approach to Advanced Membrane Structures," AIAA Paper 2001-4646, Aug. 2001.

[19] Moriya, K., and Uemura, M., "An Analysis of the Tension Field After Wrinkling in Flat Membrane Structure," *Proceedings of 1971 IASS Pacific Symposium Part II on Tension Structures and Space Frames*, Architectural Inst. of Japan, Tokyo and Kyoto, Japan, 1972, pp. 189–198.

[20] Liu, X., Jenkins, C. H., and Shur, W. W., "Large Deflection Analysis of Pneumatic Envelopes Using a Penalty Parameter Modified Material Model," *Finite Elements in Analysis and Design*, Vol. 37, No. 3, 2001, pp. 233–251. doi:10.1016/S0168-874X(00)00040-8

[21] Fujikake, M., Kojima, O., and Fukushima, S., "Analysis of Fabric Tension Structures," *Computers and Structures*, Vol. 32, Nos. 3–4, 1989, pp. 537–547. doi:10.1016/0045-7949(89)90345-3

[22] Miyazaki, Y., and Nakamura, Y., "Dynamic Analysis of Deployable Cable-Membrane Structures with Slackening Members," *Proceedings of 21st International Symposium on Space Technology and Science*, Japan Society for Aeronautical and Space Sciences, Omiya, Japan, 1998, pp. 407–412.

[23] Ding, H., Yang, B., Lou, M., and Fang, H., "New Numerical Method for Two-Dimensional Partially Wrinkled Membranes," *AIAA Journal*, Vol. 41, No. 1, 2003, pp. 125–132.

[24] Ding, H., and Yang, B., "The Modeling and Numerical Analysis of Wrinkled Membranes," *International Journal for Numerical Methods in Engineering*, Vol. 58, No. 12, 2003, pp. 1785–1801. doi:10.1002/nme.832

[25] Stein, M., and Hedgepeth, J. M., "Analysis of Partly Wrinkled Membranes," NASA TN D-813, July 1961.

[26] Mikulas, M. M., "Behavior of a Flat Stretched Membrane Wrinkled by the Rotaion of an Attatched Hub," NASA TN D-2456, Sept. 1964.

[27] Contri, P., and Schrefler, B. A., "A Geometrically Nonlinear Finite Element Analysis of Wrinkled Membrane Surfaces by a No-Compression Material Model," *Communications in Applied Numerical*

Methods, Vol. 4, No. 1, 1988, pp. 5–15.
doi:10.1002/cnm.1630040103

[28] Pipkin, A. C., "The Relaxed Energy Density for Isotropic Elastic Membranes," *IMA Journal of Applied Mathematics*, Vol. 36, No. 1, 1986, pp. 85–99.
doi:10.1093/imamat/36.1.85

[29] Steigmann, D. J., and Pipkin, A. C., "Finite Deformation of Wrinkled Membranes," *Quarterly Journal of Mechanics and Applied Mathematics*, Vol. 42, No. 3, 1989, pp. 427–440.
doi:10.1093/qjmam/42.3.427

[30] Jenkins, C. H., and Leonard, J. W., "Dynamic Wrinkling of Viscoelastic Membranes," *Journal of Applied Mechanics*, Vol. 60, Sept. 1993, pp. 575–582.

[31] Haseganu, E., and Steigmann, D. J., "Analysis of Partly Wrinkled Membranes by the Method of Dynamic Relaxation," *Computational Mechanics*, Vol. 14, No. 6, 1994, pp. 596–614.
doi:10.1007/BF00350839

[32] Baginski, F., and Collier, W., "Modeling the Shapes of Constrained Partially Inflated High-Altitude Balloons" *AIAA Journal*, Vol. 39, No. 9, 2001, pp. 1662–1672.

[33] Epstein, M., and Forcinito, M., "Anisotropic Membrane Wrinkling: Theory and Analysis," *International Journal of Solids and Structures*, Vol. 38, Nos. 30–31, 2001, pp. 5253–5272.
doi:10.1016/S0020-7683(00)00346-2

[34] Wu, C. H., and Canfield, T. R., "Wrinkling in Finite Plane-Stress Theory," *Quarterly of Applied Mathematics*, Vol. 39, July 1981, pp. 179–199.

[35] Roddeman, D. G., Drukker, J., Oomens, C. W. J., and Janssen, J. D., "The Wrinkling of Thin Membranes, Part 1: Theory," *Journal of Applied Mechanics*, Vol. 54, No. 4, 1987, pp. 884–887.

[36] Roddeman, D. G., Drukker, J., Oomens, C. W. J., and Janssen, J. D., "The Wrinkling of Thin Membranes, Part 2: Numerical Analysis," *Journal of Applied Mechanics*, Vol. 54, No. 4, 1987, pp. 888–892.

[37] Roddeman, D. G., "Finite-Element Analysis of Wrinkling Membranes," *Communications in Applied Numerical Methods*, Vol. 7, No. 4, 1991, pp. 299–307.
doi:10.1002/cnm.1630070408

[38] Jeong, D. G., and Kwak, B. M., "Complementarity Problem Formulation for the Wrinkled Membrane and Numerical Implementation," *Finite Elements in Analysis and Design*, Vol. 12, No. 2, 1992, pp. 91–104.
doi:10.1016/0168-874X(92)90057-J

[39] Muttin, F., "A Finite Element for Wrinkled Curved Elastic Membranes, and Its Application to Sail," *Communications in Numerical Methods in Engineering*, Vol. 12, No. 11, 1996, pp. 775–785.
doi:10.1002/(SICI)1099-0887(199611)12:11<775::AID-CNM17>3.0.CO;2-G

[40] Kang, S., and Im, S., "Finite Element Analysis of Wrinkling Membranes," *Journal of Applied Mechanics*, Vol. 64, No. 2, 1997, pp. 263–269.
doi:10.1115/1.2787302

[41] Lu, K., Accorsi, M., and Leonard, J., "Finite Element Analysis of Membrane Wrinkling," *International Journal for Numerical Methods in Engineering*, Vol. 50, No. 5, 2001, pp. 1017–1038.
doi:10.1002/1097-0207(20010220)50:5<1017::AID-NME47>3.0.-CO;2-2

[42] Schoop, H., Taenzer, L., and Hornig, J., "Wrinkling of Nonlinear Membranes," *Computational Mechanics*, Vol. 29, No. 1, 2002, pp. 68–74.
doi:10.1007/s00466-002-0326-y

[43] Nakashino, K., and Natori, M. C., "Efficient Modification Scheme of Stress–Strain Tensor for Wrinkled Membranes," *AIAA Journal*, Vol. 43, No. 1, 2005, pp. 206–215.
doi:10.2514/1.7143

[44] Nakashino, K., and Natori, M. C., "Three-Dimensional Analysis of Wrinkled Membranes Using Modification Scheme of Stress–Strain Tensor," *AIAA Journal*, Vol. 44, No. 7, 2006, pp. 1498–1504.
doi:10.2514/1.12052

[45] Miyazaki, Y., "Wrinkle/Slack Model and Finite Element Dynamics of Membrane," *International Journal for Numerical Methods in Engineering*, Vol. 66, No. 7, 2006, pp. 1179–1209.
doi:10.1002/nme.1588

[46] Polak, E., *Computational Methods in Optimization*, Academic Press, New York, 1971, pp. 127–133.

[47] Blandino, J. R., Johnston, J. D., and Dharamsi, U. K., "Coner Wrinkling of a Square Membrane Due to Symmetric Mechanical Loads," *Journal of Spacecraft and Rockets*, Vol. 39, No. 5, 2002, pp. 717–724.

[48] Tessler, A., Sleight, D. W., and Wang, J. T., "Effective Modeling and Nonlinear Shell Analysis of Thin Membranes Exhibiting Structural Wrinkling," *Journal of Spacecraft and Rockets*, Vol. 42, No. 2, 2005, pp. 287–298.
doi:10.2514/1.3915

J. Samareh
Associate Editor